Mechanical overload resulted in a significant increase in phosphorylated mTOR (Figures 4A and 4B) and total mTOR (Figures 4A and 4C), but no significant differences between mouse strains were noted. No significant strain by treatment effect was evident in phosphorylated or total mTOR protein levels.

Figure 4

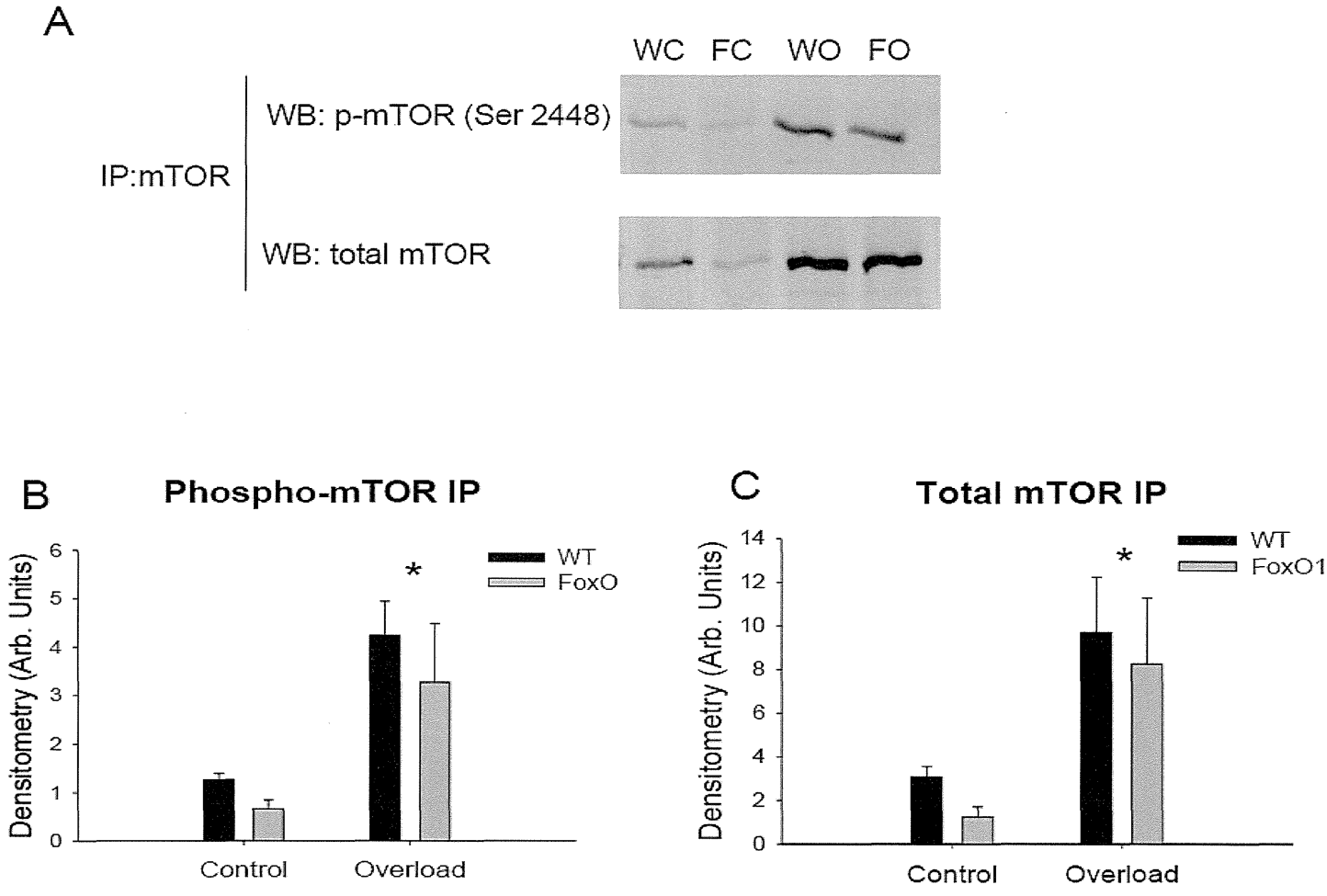

Figure 4. Immunoprecipitated Phosphorylated and Total mTOR Protein in Control and Overloaded Plantaris Muscles of Wildtype and FoxO1$^{+/-}$ Mice. Panel A: Representative western blot (WB) analyses of immunoprecipitated (IP) phosphorylated (p-mTOR) and total mTOR protein from wildtype control (WC), FoxO1$^{+/-}$ control (FC), wildtype ablation (WO) and FoxO1$^{+/-}$ ablation (FO) conditions. Panels B and C: Quantification of western blot data for phosphorylated and total mTOR, respectively. * significant main effect for treatment. $P<0.05$ for all significant differences. n=3 for all groups. Data represented as means ± standard error.

Phosphorylated (Figures 5A and 5B) and total (Figures 5A and 5C) $p70^{s6k}$ were significantly elevated in plantaris muscles following mechanical overload compared to control muscle though no overall differences between WT and $FoxO1^{+/-}$ mice were apparent. As with the upstream proteins, no strain by treatment effect was noted in phosphorylated or total $p70^{s6k}$.

Figure 5

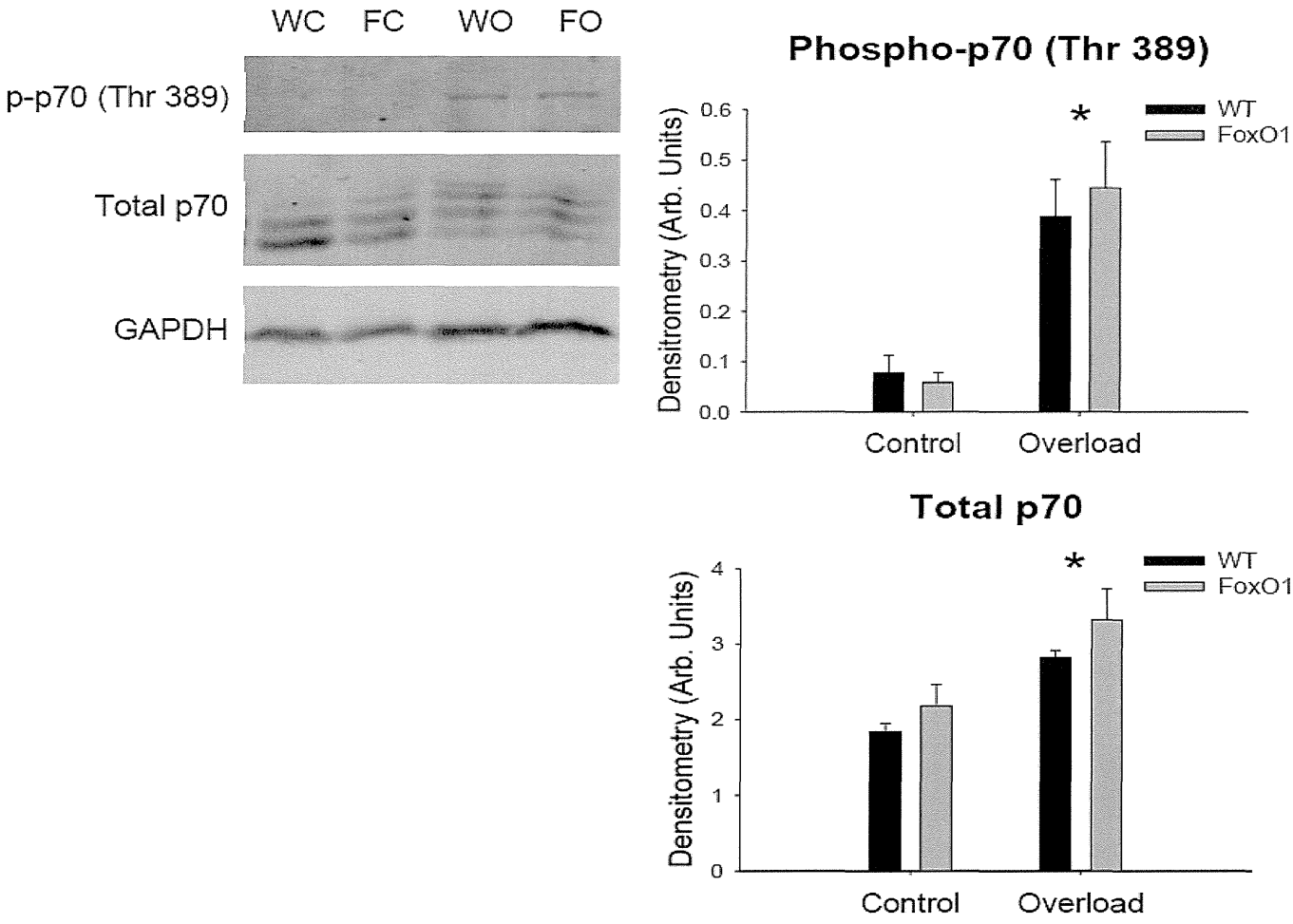

Figure 5. Phosphorylated and Total $p70^{s6k}$ Protein in Control and Overloaded Plantaris Muscles of Wildtype and $FoxO1^{+/-}$ Mice. Panel A: Representative western blot analyses from wildtype control (WC), $FoxO1^{+/-}$ control (FC), wildtype ablation (WO) and $FoxO1^{+/-}$ ablation (FO) conditions. Panels B and C: Quantification of western blot data for phosphorylated and total $p70^{s6k}$, respectively. *, significant main effect for treatment. $P<0.05$ for all significant differences. n=6 for all groups. Data represented as means ± standard error.

Phosphorylated 4EBP-1 had a tendency to be elevated in the muscles of FoxO1$^{+/-}$ mice (P=0.09; Figures 6A and 6B). However, when expressed as a ratio of total:phosphorylated protein, any potential difference was eliminated (Figure 6D). Mechanical overload resulted in significantly decreased total 4EBP-1 protein expression (Figure 6C) and the difference remained significant when expressed as the total:phosphorylated ratio (Figure 6D).

Figure 6

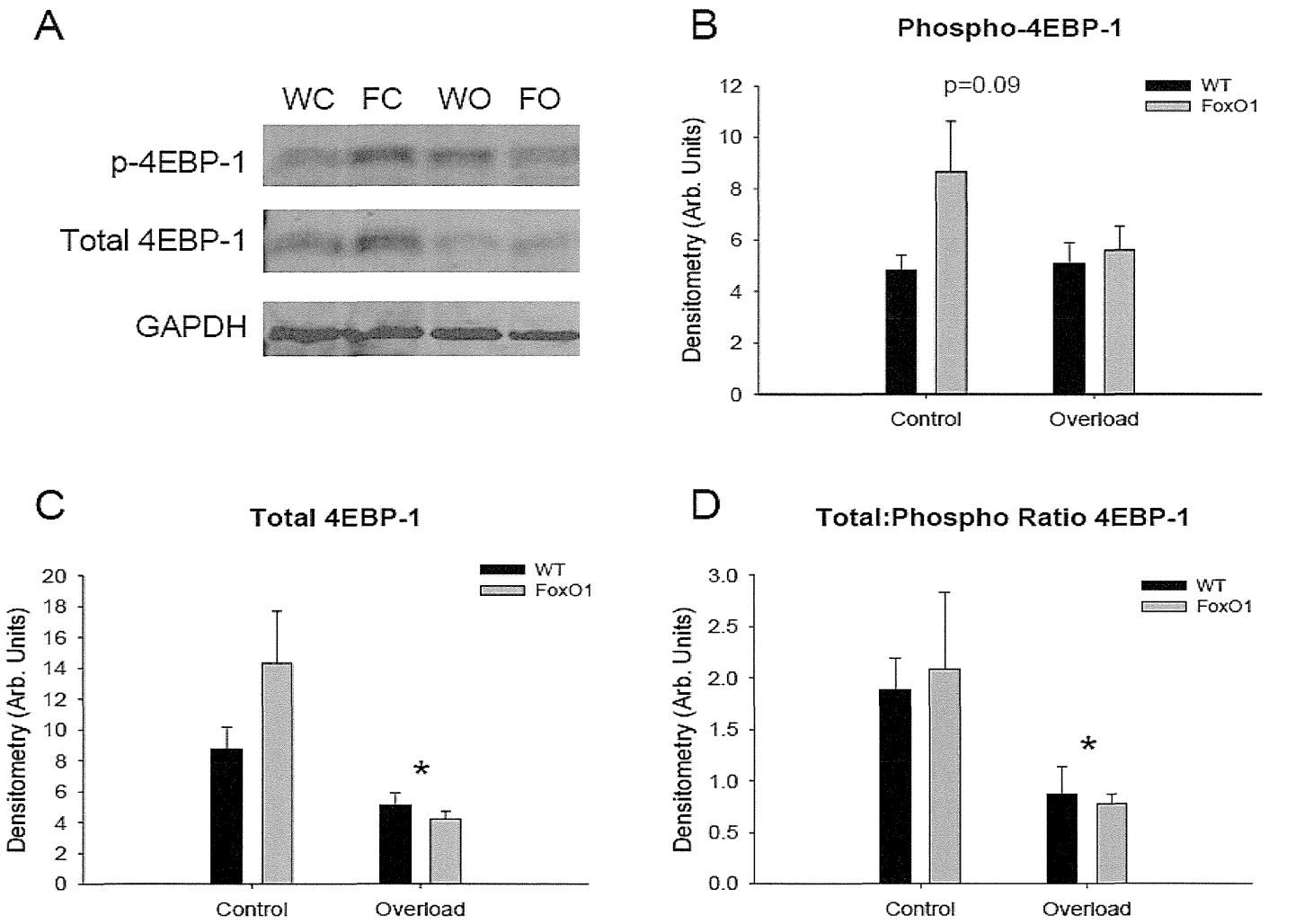

Figure 6. Phosphorylated and Total 4EBP-1 Protein in Control and Overloaded Plantaris Muscles of Wildtype and FoxO1$^{+/-}$ Mice. Panel A: Representative western blot analyses from wildtype control (WC), FoxO1$^{+/-}$ control (FC), wildtype ablation (WO) and FoxO1$^{+/-}$ ablation (FO) conditions. Panels B and C: Quantification of western blot data for phosphorylated and total 4EBP-1, respectively. Panel D: Total:phosphorylated 4EBP-1 ratio. &, trend for significant main effect for strain (P=0.09); *, significant main effect for treatment. P<0.05 for all significant differences. n=6 for all groups. Data represented as means ± standard error.

FoxO1-mediated inhibition of muscle hypertrophy is associated with elevations in MAFbx/atrogin-1 gene and protein expression. MAFbx/atrogin-1 gene expression was globally elevated in FoxO1$^{+/-}$ mice compared to WT mice and mechanical overload resulted in a significant decrease in MAFbx/atrogin-1 gene expression compared to control muscle (Figure 7A). Protein levels of MAFbx/atrogin-1 were not globally different between mouse strains; however, mechanical overload resulted in significant reductions in MAFbx/atrogin-1 protein expression in FoxO1$^{+/-}$ and WT mice compared to their respective controls (Figure 7B and 7C). Further, FoxO1$^{+/-}$ control samples displayed significantly elevated MAFbx/atrogin-1 protein compared to all other groups. Although MAFbx/atrogin-1 gene expression was globally elevated in FoxO1$^{+/-}$, total protein ubiquination was not different between strains and did not appear to change after overload (Figure 7D).

Figure 7

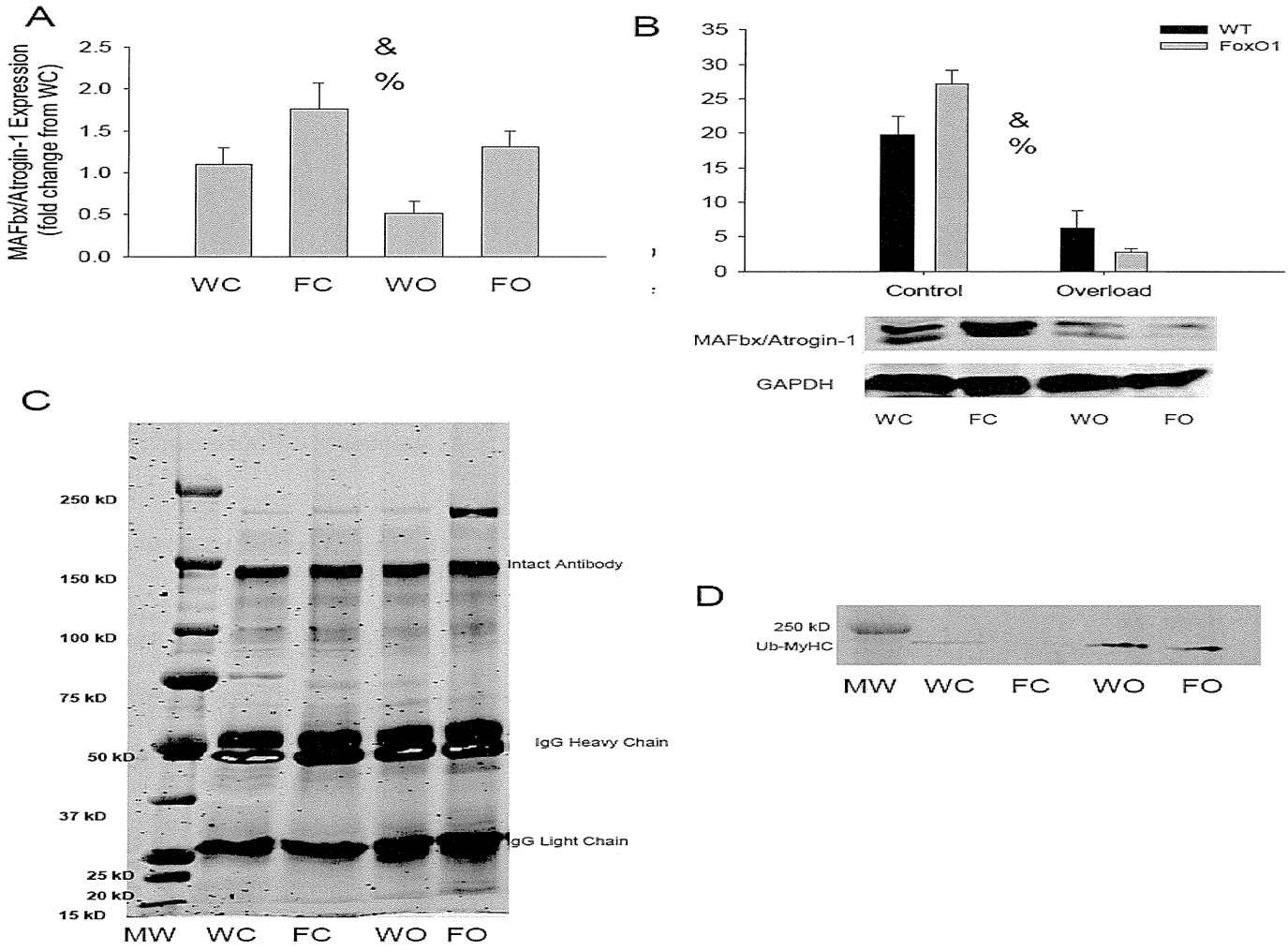

Figure 7. MAFbx/Atrogin-1 Gene Expression and Protein Ubiquination in Control and Overloaded Plantaris Muscles of Wildtype and FoxO1$^{+/-}$ Mice. (A) MAFbx/Atrogin-1 gene expression, (B) Ubiquinated myosin heavy chain, and (C) Krypton stain for total protein ubiquination. Lanes identified as wildtype control (WC), FoxO1$^{+/-}$ control (FC), wildtype ablation (WO) and FoxO1$^{+/-}$ ablation (FO) conditions. &, significant main effect for strain; %, significant main effect for treatment. $P<0.05$ for all significant differences. n=4-6 for all groups. Data represented as means ± standard error.

DISCUSSION

The findings from this study demonstrate that FoxO1 overexpression in skeletal muscle suppresses muscle hypertrophy. Markers of muscle hypertrophy including, total protein content, muscle mass, and muscle fiber cross-sectional area increased following 2 wks of mechanical overload. However, FoxO1 overexpression in skeletal muscle resulted in a dampened response compared to the observed increases in age-matched wildtype animals. Opposite our hypotheses, the above noted differences between mouse strains do not appear to be a result of quelled anabolic signaling through Akt, mTOR or the associated downstream targets as no evident changes in phosphorylation status of these proteins was detected. Additionally, the subdued response in hypertrophy observed with overexpression of FoxO1 does not appear to be caused by an increase in catabolic activity of the E3 ubiquitin ligase MAFbx/Atrogin-1. Although proteolytic machinery was likely enhanced as a result of increased FoxO1 expression, (globally higher MAFbx/atrogin-1 gene and protein expression in FoxO1 overexpressing mice), mechanical overload significantly reduced MAFbx/atrogin-1 gene and protein expression in both mouse strains to a similar degree and there was no effect of FoxO1 overexpression on protein ubiquination. As such, our contention is that the decreased muscle size conferred through FoxO1 overexpression is independent of signaling through the canonical Akt/mTOR pathway.

The balance between protein synthesis and protein degradation pathways in skeletal muscle hypertrophy was recently examined by Stitt et al.(32) in which they showed that activation of Akt was associated with a downregulation of the noted protein ubiquination genes, MuRF-1 and MAFbx/atrogin-1 in cultured muscle cells. Interestingly, the supression in MuRF-1 and MAFbx/atrogin-1 expression appeared to be largely mediated through FoxO1 as introduction of mutant FoxO1 that is not responsive to Akt signaling prevented Akt-mediated suppression of MuRF-1 and MAFbx/atrogin-1 gene activity (32). The link between FoxO transcription factors and muscle size regulation has been further substantiated through in vitro analyses using genetic downregulation models. Specifically, Sandri et al. (31) reported that muscle atrophy induced through serum starvation or glucocorticoid administration was associated with reductions in Akt-mediated signaling and promotion of MAFbx/atrogin-1 gene expression. The increased MAFbx/atrogin-1 gene expression was signficantly blunted via blockade of FoxO activity (FoxO3a; closely related FoxO homologue) through induction of dominant negative forms of FoxO or infusion of inhibitor RNA directed against FoxO. Findings by Kamei et al. (16), using a transgenic mouse model with skeletal muscle specific overexpression of the FoxO1 protein, corrorobrates these in vitro findings by demonstrating that FoxO1 supresses skeletal muscle size and increases the expression of various pro-catabolic genes (e.g., MAFbx/atrogin-1, cathepsin L).

Considering this apparent relationship between FoxO1 and skeletal muscle size and the influence of the Akt and mTOR-mediated signaling on increasing protein synthesis efficiency and/or capacity (9, 17,23,24) and regulation of genes known to boost protein ubiquination and proteosome mediated degradation (16,31,32), our work has focused on investigating the impact of FoxO1 overexpression on the activity of the major components within this complex signaling pathway. Opposite our expectations, overexpression of FoxO1 in skeletal muscle resulted in an enhanced degree of basal level Akt phosphorylation (i.e., non-overloaded muscle) compared to wildtype controls. Interestingly, recent work in multiple cell lines (7) cardiomyocytes (25) has shown that FoxO overexpression results in increases in basal Akt phosphorylation, corroborating our data. Furthermore, Moylan et al. (22) recently reported that Akt phosphorylation was significantly elevated in mouse skeletal muscle cells in vitro in the presence of the known atrophy inducing molecule TNFα. Thus, in keeping with these findings, it appears that muscle atrophy induced through FoxO1 expression occurs not as a result of suppressed Akt activity, but despite enhanced Akt signaling.

Downstream of Akt, mTOR has been shown to be the primary kinase responsible for regulating $p70^{s6k}$ (Thr 389) and 4EBP-1(Thr 37/46) phosphorylation in response to growth stimulus (9,13,23,24). mTOR is found in two protein complexes: TORC1 (mTOR, GßL/LST8, raptor, rheb), which is important for cell growth and TORC2 (mTOR, GßL, rictor), which is involved in cytoskeleton orgranization (33). Recent work by Wu et al. (34) has suggested that overexpression of FoxO1 in myocytes results in suppression of myotube formation. This is due primarily to degradation of certain components of the TORC1 complex and downstream molecular targets, specifically mTOR and $p70^{s6k}$, while other downstream targets, namely Akt and 4EBP-1, remained unchanged (34). Contrary to these findings, our current work suggests that the activity of the purported anabolic mTOR and $p70^{s6k}$ were not attenuated by FoxO1 overexpression when challenged with a growth stimulus. Further, although 4EBP-1 phosphorylation had a tendency to be elevated in the control muscle with FoxO1 overexpression, when expressed as a total: phosphorylation ratio there was no significant effect of FoxO1. Additionally, no overt changes in 4EBP-1 gene expression were found indicating that any potential differences in protein abundance observed were likely the result of post-translational mechanisms.

While $p70^{s6k}$ and 4EBP-1 have received much attention in the realm of regulating skeletal muscle mass there remains controversy as to the significance of their contribution to muscle growth. Although evidence points to the ability of $p70^{s6k}$ to phosphorylate the S6 protein on the 40S ribosomal subunit and subsequently promote protein translation initiation (23,27), cell growth is not always associated with the upregulation of $p70^{s6k}$ as research using genetic manipulations (e.g., $p70^{s6k}$ knockouts) demonstrate cell growth in the absence of $p70^{s6k}$ production (27,33). Furthermore, suggestions that ribosomal S6 acts primarily in the translation of 5' TOP mRNAs upon activation by $p70^{s6k}$ (15) appears controversial, as more recent findings suggest that mutation of S6 phosphorylation sites significantly decreases muscle size but does not impact translation of 5' TOP mRNAs, nor does it suppress protein synthesis (29). In addition, 4E-BP1, an inhibitory binding partner to the eukaryotic initiation factor 4E, has been linked to muscle size regulation as its inactivation has been widely observed in both in vitro and in vivo models of cell growth (1,2,26) and has been linked to the promotion of skeletal muscle protein synthesis (2). Although a role of 4EBP-1 in skeletal muscle size regulation has been shown, as TORC1-mediated phosphorylation of 4E-BP1 results in the subsequent release of eIF4E and formation of the eIF4F-eIF4G complex necessary for translation initiation (2), a clear understanding is still lacking. Additional studies show that blocking the formation of the eIF4F complex does not appear to blunt muscle protein synthesis or mRNA translation (14) and the expression of eIF4E does not rescue muscle cells from atrophy associated with suppression in $p70^{s6k}$ activity (1,26). It is possible that 4E-BP1 regulation of the eIF4F formation may not play a primary role during skeletal muscle hypertrophy.

Our data, taken with the literature, suggests that lack of significant findings in the activity of these signaling molecules associated with Akt and mTOR-mediated signaling may not be surprising given their controversial role in supporting the growth of skeletal muscle. Importantly, the characterized differences in fiber type and running wheel activity of FoxO1 overexpressing mice should be noted. Kamei et al. reported that FoxO1 and associated isoforms (e.g., FoxO3a) have been shown to induce muscle atrophy through induction of genes regulating protein ubiquination and proteasome mediated degradation (16,31,32). As such, we addressed MAFbx/atrogin-1 gene and protein expression and associated protein ubiquination as a potential indicator of protein degradation within skeletal muscle. As reported previously (20), MAFbx/atrogin-1 gene expression was significantly reduced (~50%) following 2-wks of chronic overload, which was consistent with our findings in both the wildtype and FoxO1 overexpressing muscle. In addition, protein levels mirrored the gene expression data as mechanical overload resulted in a reduction of MAFbx/atrogin-1 protein expression compared to control. Thus, despite the significant increase in MAFbx/atrogin-1 gene and protein expression

conferred through FoxO1 expression under basal conditions, the influence of mechanically overloading the muscle resulted in attenuation in MAFbx/atrogin-1 activity.

Moreover, our data has revealed that protein ubiquination appeared unaltered through FoxO1 overexpression. Though muscle mass was lower in control and overloaded muscle of FoxO1 mice, active protein ubiquination does not appear to be the main factor mediating the reduced degree of muscle growth observed. Importantly, previous research has predominantly studied acute muscle atrophy occurring in the hours to days following FoxO1 activation in isolated cell culture environments. Thus, it is possible that in this model of chronic FoxO1 overexpression, degradatory responses may have already culminated resulting in a new set point for muscle mass. Also, it is possible that some mechanisms may be in place within the cell to counteract continued ubiquination and potential degradation of cytoskeletal components conferred through FoxO1 expression. Alternatively, due to the rapid nature in which ubiquinated proteins are degraded by the proteasome, it is possible that FoxO1 overexpression may have amplified the rate of ubiquination and subsequent protein degradation within the muscle that was not captured in the ubiquination assay. Although not significant in control muscle in either mouse strain, MyHC ubiquination was elevated during muscle overload, which occurred concomitantly with an increase in muscle mass and cross sectional area in both mouse strains. This response is not entirely unexpected bearing in mind the rate of protein turnover in exercising muscle and the degree of protein degradation which has been observed in this surgical overload model (10). Further, using a human skeletal muscle hypertrophy model, Leger et al. (19) reported an increased phosphoryation of Akt and mTOR along with nuclear exclusion of FoxO1 in the weeks following resistance training. However, gene expression of MAFbx/atrogin-1 was significantly elevated despite marked increases in muscle cross sectional area (10%). Although the apparent differences between the studies may reflect species variability, differences in hypertrophy induction, and/or time of sampling tissues, it is conceivable that increases in certain pro-catabolic processes may be an integral part in ultimately facilitating skeletal muscle growth. Regardless, FoxO1 overexpression did not appear to differentially regulate MyHC ubiquination during mechanical overload, suggesting that gross loss of contractile elements was not a causative agent of the growth inhibition observed.

CONCLUSION

Overexpression of FoxO1 in skeletal muscle has a strong influence in suppressing skeletal muscle growth. Although the mechanism for this action remains largely elusive, it is unlikely that this suppression in growth is mediated through modulating mTOR and downstream signaling directly. However, further research, specifically experiments focused on the outcome measure of protein synthesis, is necessary to substantiate the ability of FoxO1 to impact anabolism in skeletal muscle. Further research into the mechanisms of action related to FoxO1 in skeletal muscle may provide breakthrough therapies for the treatment of muscle dysfunction associated with diseases of major social impact, such as cardiovascular disease, renal disease, pulmonary disorders, and diabetes.

ACKNOWLEDGMENTS

Supported by a grant through the deArce Memorial Endowment Fund in Support of Medical Research and Development (TJM). The authors wish to thank Zachary Brinkman and Evan Schick for their support with western blot analyses and gene expression assays.

Address for correspondence: Rachael A. Potter, Department of Kinesiology, The University of Toledo, Toledo, Ohio, 43606; Phone: 419-530-2690; Email: Rachael.Hoover@Rockets.utoledo.edu

REFERENCES

1. Anthony JC, Anthony TG, Kimball SR, Vary TC, Jefferson LS. Orally administered leucine stimulates protein synthesis in skeletal muscle of postabsorptive rats in association with increased eIF4F formation. ***J Nutr.*** 2000;130:139-145.

2. Anthony JC, Yoshizawa F, Anthony TG, Vary TC, Jefferson LS, Kimball SR. Leucine stimulates translation initiation in skeletal muscle of postabsorptive rats via a rapamycin-sensitive pathway. ***J Nutr.*** 2000;130:2413-2419.

3. Baar K, Esser K. Phosphorylation of p70(S6k) correlates with increased skeletal muscle mass following resistance exercise. ***Am J Physiol.*** 1999;276:C120-127.

4. Bodine SC, Latres E, Baumhueter S, Lai VK, Nunez L, Clarke BA, Poueymirou WT, Panaro FJ, Na E, Dharmarajan K, Pan ZQ, Valenzuela DM, DeChiara TM, Stitt TN, Yancopoulos GD, Glass DJ. Identification of ubiquitin ligases required for skeletal muscle atrophy. ***Science.*** 2001;294:1704-1708.

5. Bodine SC, Stitt TN, Gonzalez M, Kline WO, Stover GL, Bauerlein R, Zlotchenko E, Scrimgeour A, Lawrence JC, Glass DJ, Yancopoulos GD. Akt/mTOR pathway is a crucial regulator of skeletal muscle hypertrophy and can prevent muscle atrophy in vivo. ***Nat Cell Biol.*** 2001;3:1014-1019.

6. Brunet A, Bonni A, Zigmond MJ, Lin MZ, Juo P, Hu LS, Anderson MJ, Arden KC, Blenis J, Greenberg ME. Akt promotes cell survival by phosphorylating and inhibiting a Forkhead transcription factor. ***Cell.*** 1999;96:857-868.

7. Chen CC, Jeon SM, Bhaskar PT, Nogueira V, Sundararajan D, Tonic I, Park Y, Hay N. FoxOs inhibit mTORC1 and activate Akt by inducing the expression of Sestrin3 and Rictor. ***Dev Cell.*** 2010;18:592-604.

8. Dreyer HC, Glynn EL, Lujan HL, Fry CS, Dicarlo SE, Rasmussen BB. Chronic paraplegia-induced muscle atrophy downregulates the mTOR/S6K1 signaling pathway. ***J Appl Physiol.*** 2008;104(1):27-33.

9. Farrell PA, Hernandez JM, Fedele MJ, Vary TC, Kimball SR, Jefferson LS. Eukaryotic initiation factors and protein synthesis after resistance exercise in rats. ***J Appl Physiol.*** 2000;88:1036-1042.

10. Goldspink DF, Garlick PJ, McNurlan MA. Protein turnover measured in vivo and in vitro in muscles undergoing compensatory growth and subsequent denervation atrophy. ***Biochem J.*** 1983;210:89-98.

11. Gomes MD, Lecker SH, Jagoe RT, Navon A, Goldberg AL. Atrogin-1, a muscle-specific F-box protein highly expressed during muscle atrophy. ***Proc Natl Acad Sci U S A.*** 2001;98: 14440-14445.

12. Hornberger TA, McLoughlin TJ, Leszczynski JK, Armstrong DD, Jameson RR, Bowen PE, Hwang ES, Hou H, Moustafa ME, Carlson BA, Hatfield DL, Diamond AM, Esser KA. Selenoprotein-deficient transgenic mice exhibit enhanced exercise-induced muscle growth. ***J Nutr.*** 2003;133:3091-3097.

13. Hornberger TA, Sukhija KB, Wang XR, Chien S. mTOR is the rapamycin-sensitive kinase that confers mechanically-induced phosphorylation of the hydrophobic motif site Thr(389) in p70(S6k). ***FEBS Lett.*** 2007;581:4562-4566.

14. Huang BP, Wang Y, Wang X, Wang Z, Proud CG. Blocking eukaryotic initiation factor 4F complex formation does not inhibit the mTORC1-dependent activation of protein synthesis in cardiomyocytes. ***Am J Physiol Heart Circ Physiol.*** 2009;296:H505-514.

15. Jefferies HB, Fumagalli S, Dennis PB, Reinhard C, Pearson RB, Thomas G. Rapamycin suppresses 5'TOP mRNA translation through inhibition of p70s6k. ***Embo J.*** 1997;16:3693-3704.

16. Kamei Y, Miura S, Suzuki M, Kai Y, Mizukami J, Taniguchi T, Mochida K, Hata T, Matsuda J, Aburatani H, Nishino I, Ezaki O. Skeletal muscle FOXO1 (FKHR) transgenic mice have less skeletal muscle mass, down-regulated Type I (slow twitch/red muscle) fiber genes, and impaired glycemic control. ***J Biol Chem.*** 2004;279:41114-41123.

17. Kubica N, Kimball SR, Jefferson LS, Farrell PA. Alterations in the expression of mRNAs and proteins that code for species relevant to eIF2B activity after an acute bout of resistance exercise. ***J Appl Physiol.*** 2004;96:679-687.

18. Latres E, Amini AR, Amini AA, Griffiths J, Martin FJ, Wei Y, Lin HC, Yancopoulos GD, Glass DJ. Insulin-like growth factor-1 (IGF-1) inversely regulates atrophy-induced genes via the phosphatidylinositol 3-kinase/Akt/mammalian target of rapamycin (PI3K/Akt/mTOR) pathway. ***J Biol Chem.*** 2005;280:2737-2744.

19. Leger B, Cartoni R, Praz M, Lamon S, Deriaz O, Crettenand A, Gobelet C, Rohmer P, Konzelmann M, Luthi F, Russell AP. Akt signalling through GSK-3beta, mTOR and Foxo1 is involved in human skeletal muscle hypertrophy and atrophy. ***J Physiol.*** 2006;576:923-933.

20. Marino JS, Tausch BJ, Dearth CL, Manacci MV, McLoughlin T, Rakyta SJ, Linsenmayer MP, Pizza FX. {beta}2 integrins contribute to skeletal muscle hypertrophy in mice. ***Am J Physiol Cell Physiol.*** 2008;295:1026-1036.

21. McLoughlin TJ, Smith SM, Delong AD, Wang H, Unterman TG, Esser KA. FoxO1 induces apoptosis in skeletal myotubes in a DNA binding-dependent manner. ***Am J Physiol Cell Physiol.*** 2009;297(3):C548-555.

22. Moylan JS, Smith JD, Chambers MA, McLoughlin TJ, Reid MB. TNF induction of atrogin-1/MAFbx mRNA depends on Foxo4 expression but not AKT-Foxo1/3 signaling. ***Am J Physiol Cell Physiol.*** 2008;295(4):C986-993.

23. Nader GA, Hornberger TA, Esser KA. Translational control: Implications for skeletal muscle hypertrophy. ***Clin Orthop Relat Res.*** 2000;403:S178-187.

24. Nader GA, McLoughlin TJ, Esser KA. mTOR function in skeletal muscle hypertrophy: Increased ribosomal RNA via cell cycle regulators. ***Am J Physiol Cell Physiol.*** 2005;289: C1457-1465.

25. Ni YG, Wang N, Cao DJ, Sachan N, Morris DJ, Gerard RD, Kuro OM, Rothermel BA, Hill JA. FoxO transcription factors activate Akt and attenuate insulin signaling in heart by inhibiting protein phosphatases. ***Proceedings of the National Academy of Sciences of the United States of America.*** 2007;104:20517-20522.

26. Ohanna M, Sobering AK, Lapointe T, Lorenzo L, Praud C, Petroulakis E, Sonenberg N, Kelly PA, Sotiropoulos A, Pende M. Atrophy of S6K1(-/-) skeletal muscle cells reveals distinct mTOR effectors for cell cycle and size control. ***Nat Cell Biol.*** 2005;7:286-294.

27. Pende M, Um SH, Mieulet V, Sticker M, Goss VL, Mestan J, Mueller M, Fumagalli S, Kozma SC, Thomas G. S6K1(-/-)/S6K2(-/-) mice exhibit perinatal lethality and rapamycin-sensitive 5'-terminal oligopyrimidine mRNA translation and reveal a mitogen-activated protein kinase-dependent S6 kinase pathway. ***Mol Cell Biol.*** 2004;24:3112-3124.

28. Rena G, Guo S, Cichy SC, Unterman TG, Cohen P. Phosphorylation of the transcription factor forkhead family member FKHR by protein kinase B. ***J Biol Chem.*** 1999;274:17179-17183.

29. Ruvinsky I, Sharon N, Lerer T, Cohen H, Stolovich-Rain M, Nir T, Dor Y, Zisman P, Meyuhas O. Ribosomal protein S6 phosphorylation is a determinant of cell size and glucose homeostasis. ***Genes Dev.*** 2005;19:2199-2211.

30. Sacheck JM, Hyatt JP, Raffaello A, Jagoe RT, Roy RR, Edgerton VR, Lecker SH, Goldberg AL. Rapid disuse and denervation atrophy involve transcriptional changes similar to those of muscle wasting during systemic diseases. ***FASEB J.*** 2007;21:140-155.

31. Sandri M, Sandri C, Gilbert A, Skurk C, Calabria E, Picard A, Walsh K, Schiaffino S, Lecker SH, Goldberg AL. Foxo transcription factors induce the atrophy-related ubiquitin ligase atrogin-1 and cause skeletal muscle atrophy. ***Cell.*** 2004;117:399-412.

32. Stitt TN, Drujan D, Clarke BA, Panaro F, Timofeyva Y, Kline WO, Gonzalez M, Yancopoulos GD, Glass DJ. The IGF-1/PI3K/Akt pathway prevents expression of muscle atrophy-induced ubiquitin ligases by inhibiting FOXO transcription factors. ***Mol Cell.*** 2004;14:395-403.

33. Wang X, Proud CG. The mTOR pathway in the control of protein synthesis. ***Physiology (Bethesda).*** 2006;21:362-369.

34. Wu AL, Kim JH, Zhang C, Unterman TG, Chen J. Forkhead box protein O1 negatively regulates skeletal myocyte differentiation through degradation of mammalian target of rapamycin pathway components. ***Endocrinology.*** 2008;149:1407-1414.

35. Zhang X, Gan L, Pan H, Guo S, He X, Olson ST, Mesecar A, Adam S, Unterman TG. Phosphorylation of serine 256 suppresses transactivation by FKHR (FOXO1) by multiple mechanisms. Direct and indirect effects on nuclear/cytoplasmic shuttling and DNA binding. ***J Biol Chem.*** 2002;277:45276-45284.

Disclaimer
The opinions expressed in **JEP**online are those of the authors and are not attributable to **JEP**online, the editorial staff or the ASEP organization.

miR-449a Contributes to Glucocorticoid-Induced CRF-R1 Downregulation in the Pituitary During Stress

Takahiro Nemoto, Asuka Mano, and Tamotsu Shibasaki

Department of Physiology, Nippon Medical School, Tokyo, 113-8602, Japan

The hypothalamic-pituitary-adrenal axis is controlled by the feedback of glucocorticoids on the hypothalamus and pituitary. Stress increases CRF, ACTH, and glucocorticoid secretion. The expression of not only CRF mRNA in the hypothalamus and proopiomelanocortin mRNA in corticotrophs, but also CRF type 1 receptor (CRF-R1) mRNA and protein on corticotrophs are downregulated through glucocorticoids. However, the mechanisms underlying the glucocorticoid-induced CRF-R1 downregulation are not fully understood. Short RNA molecules, called microRNAs (miRNAs), are posttranscriptional regulators that usually induce translational repression or gene silencing via binding to complementary sequences within target mRNAs. We hypothesized that glucocorticoids may induce the expression of miRNAs in the pituitary, which are involved in glucocorticoid-induced downregulation of CRF-R1. We found 3 miRNAs with sequences predicted to bind to the CRF-R1 3′ untranslated region (3′-UTR) by database search. Expression of 1 of these miRNAs (miR-449a) was significantly higher in the anterior pituitary of restrained rats than in that of unrestrained control rats. Expression of miR-449a was evident in many anterior pituitary cells, including corticotrophs. Although overexpression of miR-449a decreased CRF-R1 mRNA and CRF-R1 protein expression, knockdown of miR-449a attenuated dexamethasone-induced suppression of CRF-R1 mRNA and CRF-R1 protein expression in the monolayer-cultured pituitary cells. Notably, luciferase activity was significantly lower in cells cotransfected with a luciferase vector containing the CRF-R1 3′-UTR and a miR-449a vector. miR-449a expression was significantly increased by dexamethasone. Adrenalectomy attenuated restraint-induced increase in miR-449a expression in the pituitary. These results indicated that miR-449a plays an important role in stress-induced, glucocorticoid-mediated downregulation of CRF-R1 expression. (***Molecular Endocrinology* 27: 1593–1602, 2013**)

The hormones composing the hypothalamic-pituitary-adrenal (HPA) axis including corticotropin-releasing factor (CRF), ACTH, and glucocorticoids play important roles in the stress response. Stress activates the synthesis and release of hypothalamic CRF, pituitary ACTH, and adrenal glucocorticoids (1–3). Corticotrophs in the anterior pituitary are one key element in the regulatory mechanism of the HPA axis; moreover, glucocorticoids downregulate not only CRF mRNA expression in the hypothalamus but also CRF type 1 receptor (CRF-R1) and proopiomelanocortin (POMC) mRNA expression and ACTH secretion in the anterior pituitary. Acute stress downregulates CRF-R1 mRNA expression in corticotrophs. It has been reported that glucocorticoid administration decreases CRF-R1 mRNA expression and CRF binding in the anterior pituitary of rats (4–9). However, the mechanisms underlying this stress-induced CRF-R1 downregulation are not fully understood.

MicroRNAs (miRNAs) are short noncoding RNAs of 19 to 25 nucleotides and are endogenously expressed in most eukaryotes. miRNAs posttranscriptionally regulate gene expression via base pairing with the 3′-untranslated region (3′-UTR) of target mRNAs, and this binding leads either to mRNA cleavage or to translational repression (10). Such miRNAs play important roles in myriad biological processes, including organism development and

ISSN Print 0888-8809 ISSN Online 1944-9917
Printed in U.S.A.
Copyright © 2013 by The Endocrine Society
Received November 5, 2012. Accepted July 17, 2013.
First Published Online July 26, 2013

Abbreviations: ADX, adrenalectomy; bw, body weight; CRF, corticotropin-releasing factor; CRF-R, CRF receptor; HPA, hypothalamic-pituitary-adrenal; LNA, locked nucleic acid; miRNA, microRNA; POMC, proopiomelanocortin; rno, *Rattus norvegicus*; SDS, sodium dodecyl sulfate; UTR, untranslated region.

The Endocrine Society. Downloaded from press.endocrine.org by [${individualUser.displayName}] on 20 January 2014. at 21:24 For personal use only. No other uses without permission. . All rights reserved.

cell physiology (11, 12). We hypothesized that exposure to stress may induce expression of specific miRNAs that are involved in stress-induced CRF-R1 downregulation in the pituitary. To test this hypothesis, we searched sequence database to identify miRNAs predicted to bind to the CRF-R1 3′-UTR; we then examined 1) expression of these miRNAs in the pituitary of rats exposed to restraint stress and 2) the effects of overexpression or knockdown of one such miRNA (miR-449a) on CRF-R1 mRNA and CRF-R1 protein levels in the anterior pituitary cells. Furthermore, to understand the regulation of miR-449a expression in the anterior pituitary, we assessed the effects of glucocorticoids on miRNA expression in vitro and in vivo and the effect of bilateral adrenalectomy (ADX) on miRNA expression in the anterior pituitary of rats.

Materials and Methods

Animals

Wistar rats were maintained at 23°C ± 2°C with a 12-hour light, 12-hour dark cycle (lights on at 8:00 AM, off at 8:00 PM). They were allowed ad libitum access to laboratory chow and distilled water. All experimental procedures were reviewed and approved by the Laboratory Animals Ethics Review Committee of Nippon Medical School.

Restraint stress exposure

Male rats (6 weeks old) were wrapped in a flexible wire mesh (12 mm × 12 mm), and kept for 30, 60, 90, or 120 minutes between 9:00 AM and noon in an isolated room (13, 14). Rats were killed in the adjacent room immediately after stress exposure, and their trunk blood and pituitaries were collected for plasma hormone assay and mRNA and miRNA expression analyses, respectively. Nonstressed control rats were housed in a separate room from the stressed rats and were killed and sampled in the same way as restraint-stressed rats.

Dexamethasone administration

Dexamethasone (30 and 100 μg/kg body weight [bw]) or saline was injected ip into male rats (6-weeks-old). The rats were killed 1 or 2 hours after injections, and their pituitaries were removed and used for RNA extraction.

Adrenalectomy

Six-week-old male rats (n = 40) were anesthetized with pentobarbital sodium and then were bilaterally adrenalectomized (ADX); in parallel, 6-week-old male rats (n = 40) were sham-operated. All rats were returned to their home cages and immediately given a bottle of 0.9% NaCl. After a 3-day recovery, each rat was restrained as described above. Trunk blood samples were used to measure plasma corticosterone levels to confirm successful ADX.

Primary culture of pituitary cells

Six-week-old male rats (n = 30) were killed by decapitation, and each respective pituitary was removed under sterile conditions. All anterior pituitaries were collected, pooled together, and then mechano-enzymatically dispersed as described previously (15). Briefly, tissues were washed twice in PBS and then incubated at room temperature in the PBS containing 0.01% dispase (Godoshusei) with constant stirring for 30 minutes. After washing with PBS 3 times, cells were plated in 24-well plates or 60-mm dishes and cultured with DMEM/F10 HAM culture medium (Sigma-Aldrich Co) supplemented with 10% fetal bovine serum and an antibiotics/antimycotic solution (Life Technologies). The cells were subsequently allowed to attach to the plating surfaces for 4 days in a humidified 5% CO_2/95% air incubator set at 37°C. On the day of each experiment, culture media were changed. Cells were treated with CRF at concentrations ranging from 1 pg/mL to 100 ng/mL or dexamethasone at concentrations of 1, 10, or 10^2 ng/mL for 1 hour. After incubation, the cells were assayed for miRNA expression.

Cell culture

Mouse ACTHoma AtT-20 cells were obtained from the Japanese Collection of Research Biosources Cell Bank (Ibaraki, Osaka, Japan). Cells were maintained in F-10 MEM supplemented with 15% donor horse serum and 2.5% fetal bovine serum in a humidified 5% CO_2/95% air at 37°C.

miRNA overexpression and knockdown

Each miRNA overexpression vector (pmr-mCherry-rno-miR-449a or pmr-mCherry-mock) and miRNA knockdown vector (pToughDecoy-miR-449a or pToughDecoy mock) was purchased from Takara Bio. DNA fragments, which included the miRNA or decoy expression units, were then cloned into the pAxcwit2 cosmid vector (Takara Bio) (pAx-miR449a, pAx-mock, pAx-decoy-miR449a, or pAx-decoy-mock). These cosmids were used according to the manufacturer's instruction (Takara Bio) and the COS-TPC method to construct each recombinant adenovirus. Primary cultured rat anterior cells or AtT-20 cells were infected with adenovirus by adding the viruses to culture media at a 10^6 multiplicity of infection. After 48 hours, culture media were removed, and fresh medium containing dexamethasone at a concentration of 10^2 ng/mL was added to each culture; cells were then incubated for 1 hour. To check whether a recombinant adenovirus successfully infected the cells, a fluorescent microscope was used to assess red fluorescence 48 hours after transfection.

Exosome purification

Serum samples from trunk blood or culture media were centrifuged at 3000*g* and 4°C for 30 minutes to remove debris. Each 250-μL sample (serum or culture medium) was mixed with Exo-Quick exosome precipitation solution (System Bioscience, Inc) according to the manufacturer's instruction. Purified exosome samples were resuspended in ultrapure water and were then used for miRNA quantification analysis.

RNA extraction and real-time RT-PCR analysis

Total RNA was extracted from cultured pituitary cells and rat pituitaries using RNAiso Plus (Takara Bio). For miRNA expression analysis, first-strand cDNA was synthesized using 1

The Endocrine Society. Downloaded from press.endocrine.org by [${individualUser.displayName}] on 20 January 2014. at 21:24 For personal use only. No other uses without permission. . All rights reserved.

Table 1. Primer Sequences of the Studied Genes

Genes	Primers	Length (bp)	Accession Number (GenBank)
POMC	CCTCCATAGACGTGTGGAGCTG AAGGGCTGTTCATCTCCGTTG	151 (180–330)	NM_139326
CRF-R1 (CRHR1)	TCGGCTTTCATCCTACGCAAC AATTGTAGGCGGCTGTCACCA	112 (478–589)	NM_030999
IGFBP7	CACGCGTCCAATTCCCAAG TCTGAGAGCGCGTCAGCTACA	147 (761–907)	NM_001013048
GAPDH	GGCACAGTCAAGGCTGAGAATG ATGGTGGTGAAGACGCCAGTA	143 (242–384)	NM_017008

μg denatured total RNA at 37°C for 1 hour; reactions were terminated at 85°C for 5 minutes with the Mir-X miRNA First-Strand Synthesis and SYBR qRT-PCR kit (Clontech Laboratories Inc). For mRNA expression analysis, 0.5 μg denatured total RNA and PrimeScript RT reagent kit with gDNA Eraser (Takara Bio) were used to synthesize first-strand cDNA; reactions were incubated at 37°C for 15 minutes, 84°C for 5 seconds, and finally 4°C for 5 minutes. Each PCR proceeded via denaturation at 94°C for 5 seconds and annealing-extension at 60°C for 30 seconds for 40 cycles; SYBR premix Ex Taq (Takara) and specific primers for rat *POMC*, *CRF-R1*, *IGFBP7*, and *GAPDH* (Table 1) were used. To normalize each sample for RNA content, *GAPDH*, a housekeeping gene, or *U6* small nuclear RNA (Clontech) were used for mRNA and miRNA expression analyses, respectively. Diluted normal rat pituitary cDNA and the second-derivative method were used as the standard and for calculating cycle threshold values, respectively (16).

In situ hybridization and immunohistochemistry

A digoxigenin-labeled locked nucleic acid (LNA) probe against *Rattus norvegicus* (rno)-miR-449a was purchased from Exiqon. Rat pituitaries were cryosectioned, dried for 30 minutes, and then fixed in 4% paraformaldehyde. Sections were permeabilized by proteinase K (10 μg/mL) for 10 minutes at 37°C and postfixed with 4% paraformaldehyde at 4°C. Sections were acetylated in 0.25% acetic anhydride and 1.16% triethanolamine (Wako Pure Chemicals Inc) before prehybridization. Sections were prehybridized in 50% formamide hybridization buffer for 60 minutes, and then the sections were hybridized with denatured probe in 50% formamide hybridization buffer at 54°C overnight. The slides were washed in decreasing salt solutions (4×, 2×, and 0.5× saline sodium citrate). Signals were detected by antidigoxigenin-alkaline phosphatase conjugate (Roche Diagnostics GmbH) followed by detection with nitroblue tetrazolium/5-bromo-4-chloro-3-indolyl phosphate (Roche).

Upon completion of the chromogen reaction, slides were treated in 0.3% H_2O_2 for 30 minutes at room temperature; sections were then incubated in 10% normal goat serum for 20 minutes and then incubated with an antibody to β-endorphin (1:5000) for 18 hours at 4°C (17). Sections were incubated with a secondary biotinylated goat antirabbit IgG (1:200 dilution; Vector Laboratories, Inc) for 30 minutes. Sections were then incubated with an avidin-biotin-peroxidase complex (Vector) for 3 minutes at room temperature; the Vector diaminobenzidine kit (Vector) was used to visualize the antibody-peroxidase complex. When the staining had reached appropriate intensity, the tissue was rinsed in PBS, dehydrated with a graded series of alcohol solutions, cleared with xylenes, and covered with Vecta-Mount (Vector) and a coverslip. Images were captured with a microscope (AX-80; Olympus) and a color digital camera (DP72; Olympus); the cellSens software (Olympus) was then used to digitize the images.

The 3′-UTR assay

RT-PCR using forward primer (GCTAGCTGCAAGCT-CACTGACGAGCC) and reverse primer (TCTAGAGGACTG-GACCATTCTAACCC) were used to amplify a segment of CRF-R1 3′-UTR sequence (AF039203) that contained an miR-449a binding sequence from normal rat anterior pituitary RNA; this amplified segment was designated CRF-R1 3′-UTR (wt) (see Figure 3E). We also synthesized a negative control oligonucleotide with a mutant miR-449a target site. CACTGCCA was mutated to TCCACACG; additionally, the In-Fusion cloning kit (Takara Bio) was used to generated a mutant variant of the CRF-R1 3′-UTR. This variant was designated CRF-R1 3′-UTR (sc). The CRF-R1 3′-UTR fragment and the corresponding negative control variant were subcloned into pmir-GLO vector (Promega) to generate pmir-GLO-CRF-R1 3′-UTR (wt) and pmiR-GLO-CRF-R1 3′-UTR (sc), respectively (18). HEK293 cells were seeded in 60-mm dishes, and Multifectam (Promega) was used to cotransfect cells with a target plasmid (2.5 μg) (pmir-GLO-CRF-R1 3′-UTR [wt], pmir-GLO-CRF-R1 3′-UTR [sc] or pmir-GLO mock) and a miRNA plasmid (pmr-mCherry-miR-449a or pmR-mCherry mock plasmid). Cells were collected 48 hours after transfection, and the dual-luciferase reporter assay system (Promega) was used according to the manufacturer's instruction to measure enzyme activity.

Antibodies against CRF-R

Goat anti-CRF-R1 antibodies, C-20 (sc-1757), and V-14 (sc-12381), were purchased form Santa Cruz Biotechnologies, Inc. C-20 antibody recognizes both CRF-R1 and CRF-R2, but V-14 antibody recognizes only CRF-R1. We compared the quality of images with both antibodies (Figure 1F). The CRF-R1 signals on Western blots changed in parallel with the CRF-R1 mRNA signals generated via real-time PCR (Figure 1, E and H). The estimated molecular masses of CRF-R1 and CRF-R2 were almost identical (CRF-R1, 45.3 kDa; CRF-R2, 46.0 kDa) when calculated based on amino acid sequence of the processed proteins. A previous immunohistochemical study showed that the C-20 antibody resulted in strong staining in the rat pituitary, but the N-20 antibody, which is specific for CRF-R2 antibody, resulted in quite weak staining in rat pituitary; together, these findings indicate that CRF-R2 expression in rat anterior pituitary is quite

The Endocrine Society. Downloaded from press.endocrine.org by [${individualUser.displayName}] on 20 January 2014. at 21:24 For personal use only. No other uses without permission. . All rights reserved.

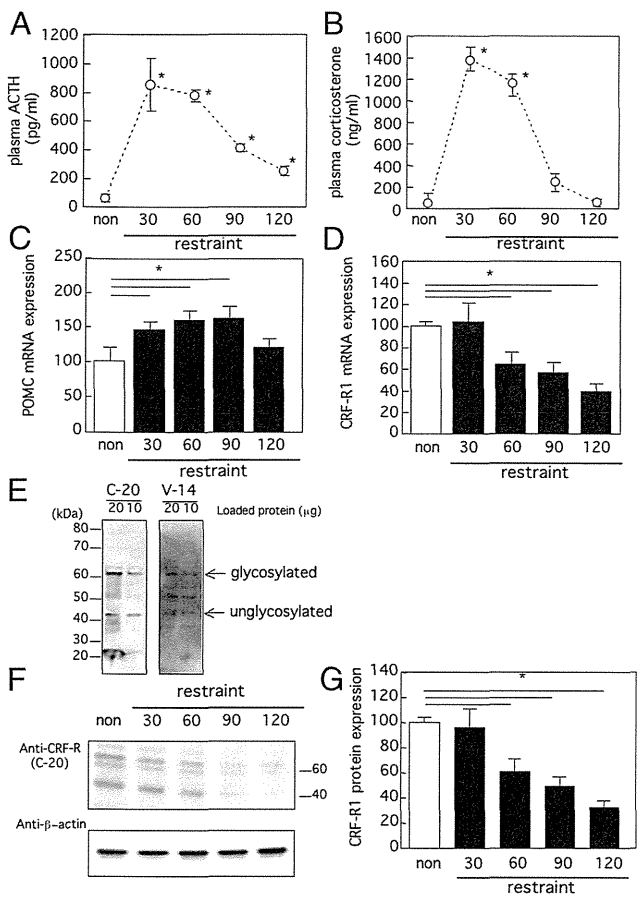

Figure 1. Plasma ACTH and corticosterone levels and POMC mRNA expression in the anterior pituitary are higher in restraint-stressed rats than in unstressed controls; in contrast, CRF-R1 mRNA and CRF-R1 protein levels in the anterior pituitary are lower in restraint-stressed rats. Rats were exposed to restraint stress for 30, 60, 90, or 120 minutes. A–D, Plasma ACTH (A) and corticosterone (B) and POMC mRNA (C) and CRF-R1 mRNA (D) in the anterior pituitary were assayed. E, Image of Western blots bearing signals from anti-CRF-R1 antibody were compared. CRF-R1 protein expression in the anterior pituitary was assayed. F, A typical image of a CRF-R1 Western blot. G, Values of these signals, determined as described in Materials and Methods. mRNA and protein expression levels are shown as percentage of nonrestrained control (non); n = 6. *, $P < .05$ vs nonrestrained control.

low (19). The C-20 antibody reportedly recognizes a glycosylated form of CRF-R1 that is approximately 60 kDa (20). On Western blots, the C-20 antibody and V-14 antibody each recognizes the same two bands; one band was probably the 40-kDa unglycosylated form of CRF-R1, and the other band was probably the 60-kDa glycosylated form of CRF-R1; these molecular masses were the same as those reported previously (20). Western blots probed with C-20 were compared with those probed with V-14; no additional band that might have corresponded to CRF-R2 was evident on the blots probed with C-20. Because the C-20 blots were clearer than the V-14 blots, we measured C-20 signals from the 60- and 40-kDa bands and used these values to represent CRF-R1.

Western blotting of CRF-R1

The anterior pituitary tissues or call lysates were lysed with Tris-Nonidet-EDTA (TNE) buffer (10mM Tris-HCl [pH 7.8], 1% Nonidet P-40, 150mM NaCl, and 1mM EDTA) containing the Complete proteinase inhibitor cocktail (Roche). Lysates were subjected to centrifugation to remove debris; and the protein concentrations in each supernatant was measured. Each sample of protein extract (20 μg) was mixed with 3× sodium dodecyl sulfate (SDS) sample buffer (200mM Tris-HCl [pH 6.8], 30% glycerol, 6% SDS, 0.03% bromophenol blue, and 3% β-mercaptoethanol); each mixture was then boiled for 5 minutes. Proteins in each sample were then separated by SDS-PAGE and transferred onto polyvinylidene difluoride membranes. The membranes were blocked with 10% nonfat dried milk and incubated with anti-CRF-R1 antibodies (1:1000). The membranes were washed and then incubated with horseradish peroxidase-conjugated antigoat IgG (Jackson ImmunoResearch Laboratory). ChemiDoc XRS (Bio-Rad Laboratories, Inc) and SuperSignal West Dura Extended Duration Substrate (Thermo Scientific) were used to detect and measure CRF-R1 immunoreactive signal. After detecting CRF-R1 signal, each membrane was incubated in restore PLUS Western blot stripping buffer (Thermo Scientific) to remove the C-20 antibodies and incubated with mouse anti-actin monoclonal antibody (Progen Biotechnik) and then horseradish peroxidase-conjugated anti-mouse IgG (Jackson ImmunoResearch). The actin immunoreactive signals were detected and measured to normalize for equal loading and blotting efficiency. CRF-R1 expression levels were calculated as follows: (intensity of 60-kDa band + intensity of 40kDa band)/intensity of actin. Data are shown as a percentage of nonstressed or control values.

Statistical analysis

A 1-way ANOVA followed by Turkey's post hoc test or 2-way ANOVA with a Bonferroni correction for multiple comparisons was used for each statistical analysis; Prism version 5.0 software (GraphPad Software, Inc) was used for all calculation. For each study involving pituitary cell culture, 2 independent replicate experiments were performed using identical protocols. For real-time RT-PCR data, all results are expressed as percentage of control values. Statistical significance was defined as $P < .05$.

Results

Restraint stress increases miR-449a expression in the anterior pituitary

Restraint stress significantly increased plasma ACTH (853.8 ± 183.5 pg/mL at 30 minutes and 775.4 ± 42.8 pg/mL at 60 minutes) and corticosterone (1385.9 ± 112.1 ng/mL at 30 minutes and 1171.1 ± 131.9 ng/mL at 60 minutes) levels. Levels of each hormone had decreased from peak levels by 90 and 120 minutes (Figure 1, A and B). Restraint stress also significantly increased POMC mRNA expression at 30 minutes (1.5 ± 0.1-fold vs nonrestrained control), at 60 minutes (1.6 ± 0.2-fold vs nonrestrained control), and at 90 minutes (1.6 ± 0.2-fold vs nonrestrained control) in the anterior pituitary (Figure 1C). The restraint stress-induced increases in POMC

The Endocrine Society. Downloaded from press.endocrine.org by [${individualUser.displayName}] on 20 January 2014. at 21:24 For personal use only. No other uses without permission. . All rights reserved.

mRNA level had subsided to baseline levels by 120 minutes. Restraint stress significantly decreased CRF-R1 mRNA expression in the anterior pituitary at 60 minutes (65.0% ± 10.7% of nonrestrained control), at 90 minutes (56.%8 ± 9.9% of nonrestrained control), and at 120 minutes (39.7% ± 6.9% nonrestrained control) (Figure 1D).

We detected CRF-R1 protein in the pituitary using anti-CRF-R1 antibodies (Figure 1E). The immunoblots produced with the C-20 antibody were clear with less background than those produced with V-14; therefore, we used the C-20 blots to measure CRF-R1 protein expression in the anterior pituitary. A representative immunoblot of CRF-R1 protein from the anterior pituitary of restrained rats is shown in Figure 1F. Restraint stress significantly decreased CRF-R1 protein expression levels at 60 minutes (61.2% ± 9.7% of nonrestrained control), at 90 minutes (49.0% ± 7.6% of nonrestrained control), and at 120 minutes (32.3% ± 5.3% of nonrestrained control) in the anterior pituitary (Figure 1G).

The miRBase (www.mirbase.org) and TargetScan (www.targetscan.org) databases were searched to identify miRNAs predicted to bind to the CRF-R1 3′-UTR. We found 3 miRNAs, rno-miR-34a (MI0000877), rno-miR-34c (MI0000876), and rno-miR-449a (MI0001650), that have sequences predicted to bind to CRF-R1 3′-UTR. Expression of miR-449a, but not of miR-34a or miR-34c, was higher in the anterior pituitaries of restraint-stressed rats than in those of unstressed rats (Figure 2, A–C); therefore, we focused on miR-449a expression. Restraint stress significantly increased miR-449a expression in the anterior pituitary (2.0 ± 0.5-fold at 30 minutes, 2.2 ± 0.2-fold at 60 minutes, 2.7 ± 0.7-fold at 90 minutes, and 2.0 ± 0.1-fold at 120 minutes vs nonrestrained control).

Expression of miR-449a in the anterior pituitary of rats

Pituitary gland tissue sections were double labeled via immunohistochemistry with anti-β-endorphin antiserum and in situ hybridization with a miR-449a LNA or a scrambled LNA negative control probe. Signals from the miR-449a LNA probe were evident in many pituitary cells, including corticotrophs that costained with anti-β-endorphin antiserum (Figure 2, D and E); in contrast, no signal from the negative control probe was evident in any cells.

Effect of miR-449a expression levels on CRF-R1 mRNA and protein expression in vitro

Overexpression of miR-449a in monolayer-cultured anterior pituitary cells significantly decreased CRF-R1

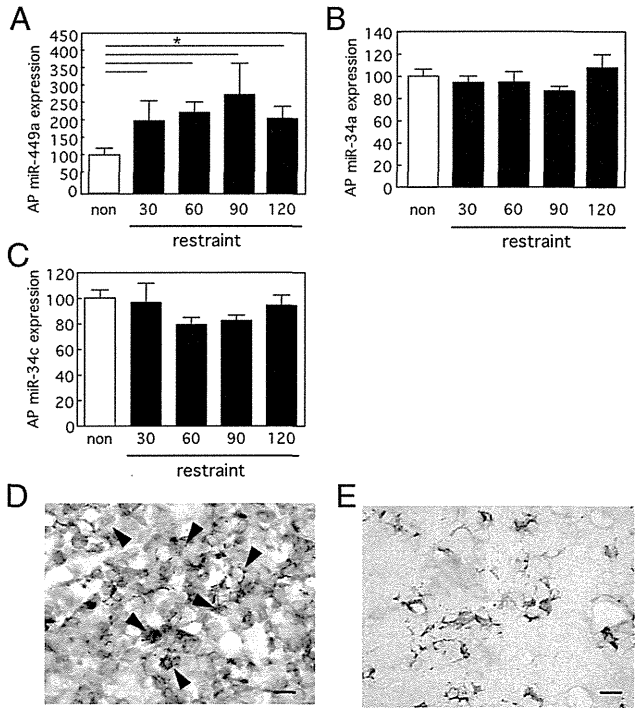

Figure 2. Restraint stress increases miR-449a expression in the anterior pituitary (AP). Rats were exposed to restraint stress for 30, 60, 90, or 120 minutes. Anterior pituitaries were assayed for miR-449a (A), for miR-34a (B), and for miR-34c (C). miRNA levels are shown as percentage of nonstressed control (non); n = 6. *, $P < .05$ vs nonrestrained control. D, Expression of miR-449a in the anterior pituitary of rats was measured. A typical micrograph of anterior pituitary tissue subjected to in situ hybridization with a miR-449a LNA probe (purple) and immunohistochemistry with anti-β-endorphin antibody (brown) is shown. Double-positive cells are indicated by arrowheads. E, Digoxigenin-labeled mutated (scrambled) LNA probe was a negative control for miR-449a signal in the anterior pituitary of rats. Scale bar, 20 μm.

mRNA expression (73.9% ± 5.2% of mock) and CRF-R1 protein expression (71.3% ± 0.9% of mock) (Figure 3, A–C); in contrast, expression of *IGFBP7* mRNA, which is reportedly expressed in corticotrophs and negatively regulated by glucocorticoids (21), was not affected by miR-449a overexpression (Figure 3D). When miR-449a was coexpressed with pmir-GLO-CRF-R1 3′-UTR in HEK293 cells, luciferase activity was significantly lower than that of mock-transfected cells (85.2% ± 1.1% for 2.5 μg and 76.2% ± 4.3% for 7.5 μg of pBA-449a transfection compared with that of pmr-GLO-mock cotransfectant), whereas there was no change in luciferase activity in cells that coexpressed miR-449a with pmr-GLO-CRF-R1 3′-UTR (sc) (Figure 3, E and F). The ToughDecoy system was used for knockdown of miR-449a expression in monolayer-cultured anterior pituitary cells (Figure 3, G–I) or in AtT-20 mouse ACTHoma cells (Figure 3, J and K); miR-449a knockdown did not increase the basal CRF-R1 mRNA and CRF-R1 protein levels in either cell type, but it did significantly attenuate

The Endocrine Society. Downloaded from press.endocrine.org by [${individualUser.displayName}] on 20 January 2014. at 21:24 For personal use only. No other uses without permission. . All rights reserved.

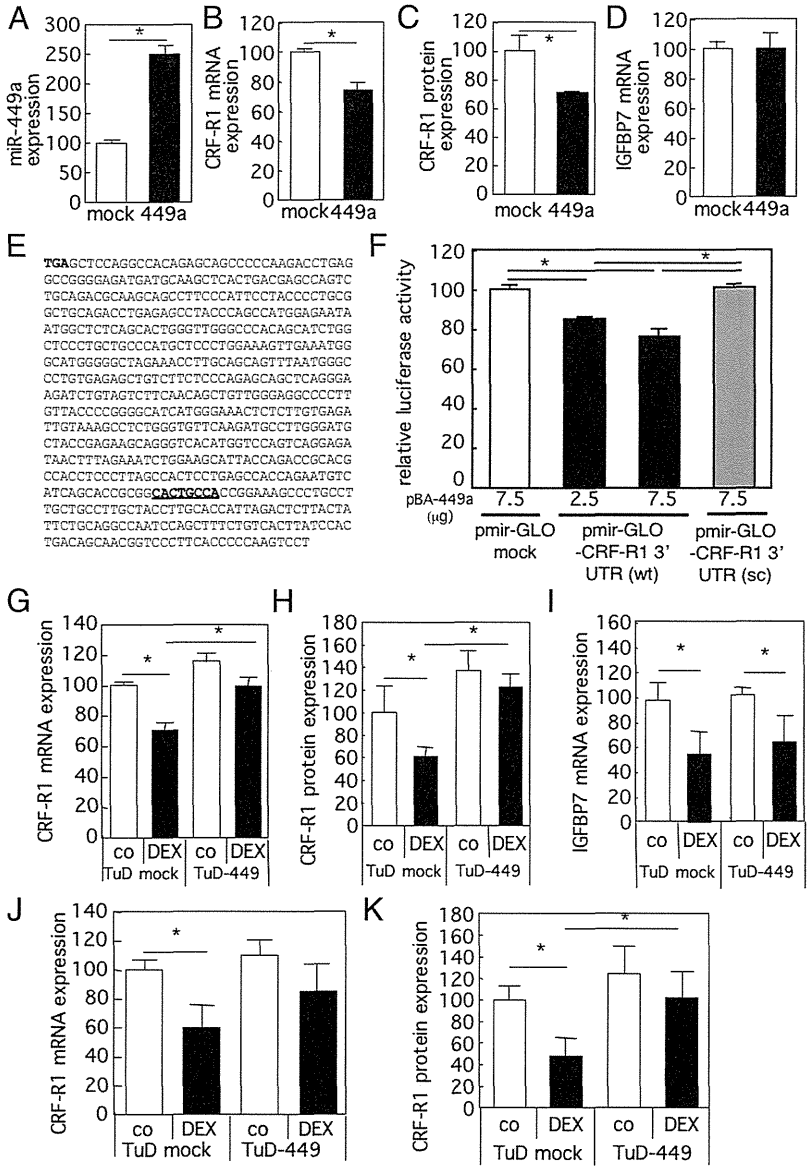

Figure 3. Effects of miR-449a expression on CRF-R1 mRNA and CRF-R1 protein expression and CRF-R1 3′-UTR luciferase reporter. Anterior pituitary cells were infected with recombinant adenovirus expressing miR-449a (pCherry 449a) or mock (pCherry mock). A–D, After 48 hours, miR-449a (A), and *CRF-R1* mRNA (B), CRF-R1 protein (C), and *IGFBP7* mRNA (D) were assayed. The levels are shown as percentage of those with pCherry mock; n = 6. *, $P < .05$ vs pCherry mock. E, The nucleotide sequence of CRF-R1 3′-UTR is shown. The miR-449a target site is underlined. The transcriptional termination codon is in bold. HEK293 cells were cotransfected with pmir-GLO-CRF-R1 3′-UTR (wt), pmir-GLO-CRF-R1 3′-UTR (sc) (which has a scrambled miR-449a target site), or pmir-GLO mock plasmid and pmr-mCherry-miR-449a (pCherry 449a). F, After 48 hours, luciferase activity in each sample was assayed. The levels of luciferase activity are shown as percentage of pmir-GLO mock; n = 6. *, $P < .05$ vs pmir-GLO mock. G–K, Cultured anterior pituitary cells (G, H, and I) and AtT-20 mouse ACTHoma cells (J and K) were infected with recombinant adenovirus expressing ToughDecoy-miR-449a (TuD-449) or mock (TuD mock). After 48 hours, expression of CRF-R1 mRNA (G and J) and protein (H and K) and IGFBP7 mRNA (I) were assayed. The levels are shown as percentage of those in saline-treated TuD mock; n = 6. *, $P < .05$ vs TuD mock. Abbreviation: co, control; DEX, dexamethasone.

the dexamethasone-induced decrease in CRF-R1 mRNA (Figure 3, G and J) and CRF-R1 protein (Figure 3, H and K) expressionsin each cell type without affecting dexamethasone-induced suppression of *IGFBP7* mRNA expression (Figure 3I).

Regulation of miR-449a expression in the anterior pituitary of rats

Treatment with dexamethasone for 1 hour significantly increased miR-449a expression at concentrations of 1 ng/mL (1.6 ± 0.1-fold), 10 ng/mL (1.7 ± 0.2-fold), and 10^2 ng/mL (2.1 ± 0.2-fold), whereas there was no change with CRF treatment in monolayer-cultured anterior pituitary cells (Figure 4A). Dexamethasone decreased CRF-R1 mRNA expression (74.6% ± 17.6% of control for 10 ng/mL and 58.1% ± 5.8% of control for 10^2 ng/mL) (Figure 4B) in vitro.

Expression of miR-449a in the anterior pituitary was significantly higher in dexamethasone-injected rats than in saline-injected control rats (2.3 ± 0.5-fold for 100 μg/kg bw at 1 hour and 2.3 ± 0.3-fold for 100 μg/kg bw at 2 hours vs saline-injected rats) (Figure 5A). Dexamethasone significantly decreased CRF-R1 mRNA expression (90.8% ± 1.0% at 1 hour, and 85.0% ± 2.9% for 30 μg/kg bw and 85.1% ± 2.3% for 100 μg/kg bw at 2 hours, of saline-injected control) (Figure 5C) and CRF-R1 protein expression (79.3% ± 2.5% of saline-injected control for 100 μg/kg bw at 2 hours) (Figure 5D) in vivo.

ADX blocked the restraint-induced increase in miR-449a expression in the anterior pituitary (Figure 6A). Although restraint stress decreased CRF-R1 mRNA expression (Figure 6B) and CRF-R1 protein expression (Figure 6C) in sham-operated and ADX rats, the restraint stress-induced decrease in CRF-R1 mRNA and protein expression was significantly diminished in ADX rats compared with those of sham-operated rats at 60, 90, and 120 minutes and at 90 and 120 minutes, respectively (Figure 6, B and C).

The Endocrine Society. Downloaded from press.endocrine.org by [${individualUser.displayName}] on 20 January 2014. at 21:24 For personal use only. No other uses without permission. . All rights reserved.

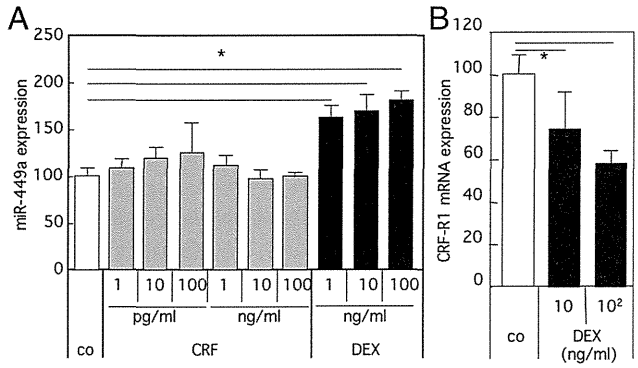

Figure 4. Dexamethasone increases miR-449a expression and decreases CRF-R1 mRNA expression in monolayer-cultured anterior pituitary cells. Primary cultured anterior pituitary cells were treated with CRF or dexamethasone (DEX) for 1 hour. A and B, Expression of miR-449a (A) and CRF-R1 mRNA (B) was assayed. miRNA and mRNA levels are shown as percentage of control; n = 8. *, $P < .05$ vs control (co).

Discussion

We found that CRF-R1 mRNA and CRF-R1 protein expression in the anterior pituitary was downregulated by restraint stress; our findings were consistent with those from previous studies (22). Glucocorticoid administration decreases not only CRF-R1 mRNA expression but also CRF-R1 protein expression (6, 23), and glucocorticoids, which are increased in response to stress, are involved in the downregulation of CRF-R1 expression during stress (3). However, the mechanisms underlying the stress-induced downregulation of CRF-R1 are not fully understood (5–7).

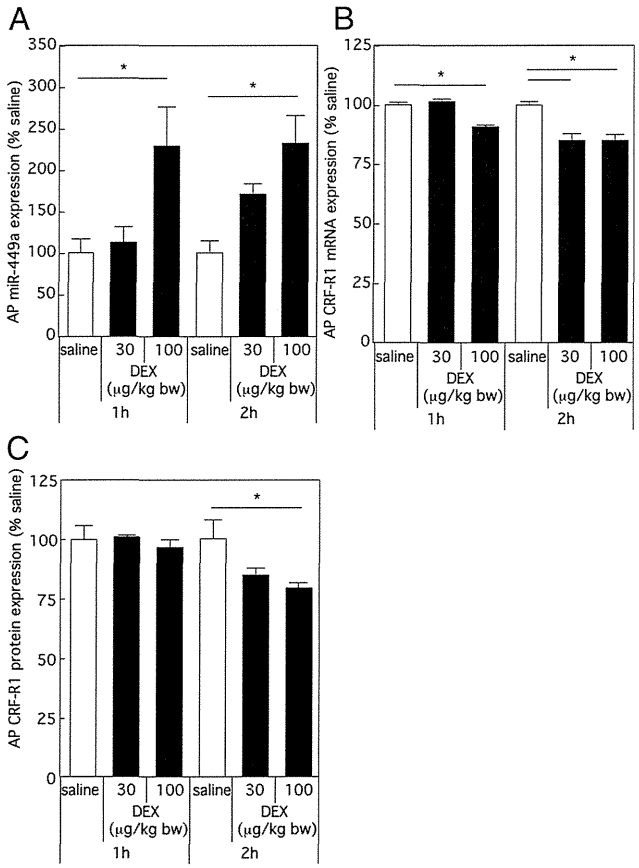

Figure 5. Dexamethasone increases miR-449a expression in the anterior pituitary and decreases CRF-R1 mRNA and CRF-R1 protein expressions in the anterior pituitary of rats. Dexamethasone or saline was injected ip into rats. A–C, Anterior pituitary miR-449a (A), CRF-R1 mRNA (B), and CRF-R1 protein (C) levels were assayed. miRNA, mRNA, and protein levels are shown as percentage of those in saline-injected rats; n = 8. *, $P < .05$ vs saline.

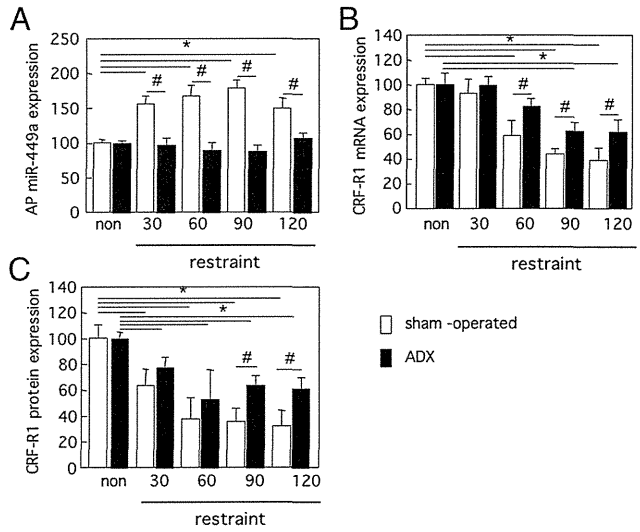

Figure 6. ADX attenuates restraint-induced miR-449a expression and suppression of CRF-R1 mRNA and CRF-R1 protein expression. ADX or sham-operated rats were restrained for 30, 60, 90, or 120 minutes. A–C, Levels of miR-449a (A) and CRF-R1 mRNA (B) and protein (C) were measured. miRNA, mRNA, and protein expression levels are shown as percentage of those in nonrestrained control (non); n = 6. *, $P < .05$ vs nonrestrained control. Abbreviation: AP, anterior pituitary.

Here, we identified 3 miRNAs (miR-449a, miR-34a, and miR-34c) that were predicted to bind to CRF-R1 3′-UTR based on database search. Expression of miR-449a, but not of miR-34a and miR-34c, was increased in the anterior pituitary of restraint-stressed rats. Overexpression of miR-449a suppressed CRF-R1 mRNA and CRF-R1 protein expression, and conversely, knockdown of miR-449a attenuated dexamethasone-induced suppression of CRF-R1 mRNA expression and CRF-R1 protein expression in monolayer-cultured rat anterior pituitary cells. The sequences of miR-449a and its binding region of CRF-R1 3′-UTR are 100% homologous among human, mouse, and rat. Furthermore, we showed that knockdown of miR-449a in AtT-20 cells also attenuated dexamethasone-induced suppression of CRF-R1 mRNA and protein expression. These results indicate that stress downregulates the expression of CRF-R1 mRNA and CRF-R1 protein through glucocorticoids and that miR-449a contributes to the glucocorticoid-induced downregulation of CRF-R1 expression in the anterior pituitary (Figure 7). However, factors other than miR-449a also seem to contribute to the glucocorticoid-induced down-

The Endocrine Society. Downloaded from press.endocrine.org by [${individualUser.displayName}] on 20 January 2014. at 21:24 For personal use only. No other uses without permission. . All rights reserved.

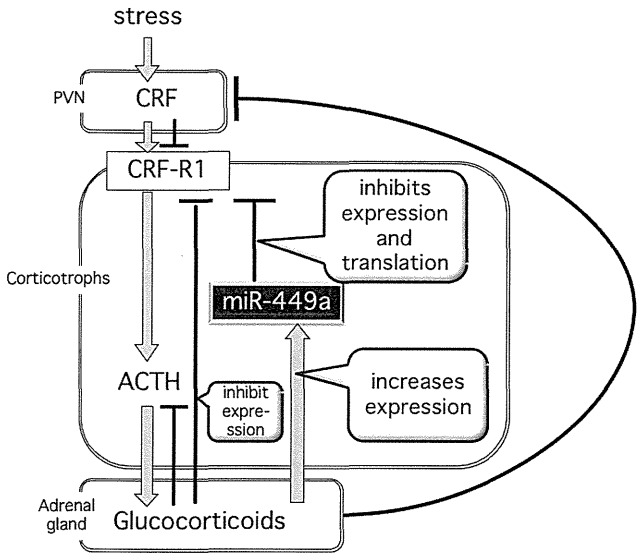

Figure 7. Proposed mechanism of stress-induced CRF-R1 downregulation. Stress activates the HPA axis. CRF from the hypothalamus stimulates ACTH secretion by corticotrophs via activated CRF-R1, and ACTH then stimulates the adrenal gland to produce glucocorticoids. The hypothalamus and pituitary hormones are regulated via negative feedback inhibition by glucocorticoids: glucocorticoids downregulate CRF mRNA expression in the paraventricular nucleus of the hypothalamus (PVN); glucocorticoids also downregulate CRF-R1 and proopiomelanocortin (POMC) mRNA expression and ACTH secretion from corticotrophs. Here, we showed that glucocorticoids increased the expression of miR-449a and that miR-449a then inhibits CRF-R1 mRNA expression and translation in the anterior pituitary of restrained rats. However, the mechanism by which glucocorticoids activate miR-449a transcription remains unclear.

regulation of CRF-R1 because the restraint stress-induced increase in miR-449a expression was completely blocked by ADX, but the restraint stress-induced decrease in CRF-R1 mRNA and protein was not completely blocked by ADX. A change in CRF-R1 mRNA stability may also be important to CRF-R1 downregulation during stress because glucocorticoids may also decrease CRF-R1 mRNA stability (8). Furthermore, because intracerebroventricular injection of CRF decreases CRF-R1 mRNA expression in the anterior pituitary of ADX rats (3), not only glucocorticoids, but also other factors, such as CRF, seem to be involved in stress-induced downregulation of CRF-R1 expression.

Transcription of all miRNAs is controlled by RNA polymerase II, and primary miRNAs are processed in the nucleus (24–26), but little is known about the signaling pathways that control miRNA expression. We did not find a glucocorticoid-responsive element near the miR-449a coding region; therefore, additional studies are needed to clarify the detail of intracellular signaling pathways leading to a glucocorticoid-induced increase in miR-449a expression.

Cells expressing CRF-R1 mRNA are widely distributed throughout the rat brain and pituitary (27, 28), but dexamethasone administration did not cause changes in CRF-R1 mRNA expression in the intermediate lobe of pituitary or in brain regions such as frontal cortex, olfactory bulb, and amygdala (7). Our double-labeling technique involving in situ hybridization and immunohistochemistry showed that miR-449a was widely expressed in many pituitary cells, including corticotrophs. Taken together with previous published results, our current results indicated that glucocorticoid-induced downregulation of CRF-R1 may involve miR-449a only in anterior pituitary cells. Recent findings have revealed that miRNAs inhibit expression of many types of receptors: miR-133b inhibits epidermal growth factor receptor (29), miR-126 inhibits vascular endothelial growth factor receptor 2 (30), let-7b inhibits GH receptor (31), and miR-376a and miR-376c inhibit IGF-1 receptor (32). However, little is known about the physiological role of miRNAs in expression of pituitary hormone receptor. The current study provides new insight into understanding the function of miRNAs in the regulation of the HPA axis response to stress.

The miRNA identified in this study, miR-449a, has not been thoroughly studied. However, several research groups have demonstrated that human miR-449a acts as a tumor suppressor in prostate, bladder, and lung cancers (33–35). In general, each miRNA has multiple target genes (36). Actually, rat miR-449a has approximately 500 potential target genes based on analysis of the TargetScan database. Additional studies are needed to further clarify the roles of miR-449a that do not involve CRF-R1 suppression in corticotrophs.

Recent findings show that miRNAs are released from cells in small vesicles, which are called exosomes, and that exosomal miRNAs are stable in blood and in extracellular fluids (37, 38). We detected miR-449a not only in the anterior pituitary cells but also in exosomes in culture medium of pituitary cells and in serum of rats (data not shown). Serum exosomal miR-449a increased in parallel with miR-449a mRNA expression in the anterior pituitary of restrained rats. Because miR-449a is expressed in the brain and various peripheral tissues (39), the origin of serum exosomal miR-449a is unclear. However, the anterior pituitary could be one site of origin of the miR-449a–containing exosomes found in peripheral circulation because exosomal miR-449a in serum and exosomal miR-449a in culture media increased during restraint stress and after dexamethasone treatment, respectively. Exosomes carry proteins, RNAs, and miRNAs; they are released into extracellular fluids, and they mediate cell-to-cell signaling in a paracrine manner (40); therefore, miR-449a–containing exosomes may have a paracrine role in the anterior pituitary. Moreover, because sequences of miR-449a and miR-449a target sequences in

The Endocrine Society. Downloaded from press.endocrine.org by [${individualUser.displayName}] on 20 January 2014. at 21:24 For personal use only. No other uses without permission. . All rights reserved.

CRF-R1 3′-UTR are 100% identical between human and rats, measuring exosomal miR-449a in serum is probably practicable and may provide new insights into the pathophysiology of stress-related disease in humans.

In summary, our findings indicate that pituitary miR-449a has an important role in glucocorticoid-induced downregulation of CRF-R1 mRNA expression and CRF-R1 protein expression in the corticotrophs of the anterior pituitary in stressed rats.

Acknowledgments

Address all correspondence and requests for reprints to: Dr Takahiro Nemoto, Department of Physiology, Nippon Medical School, 1-1-5, Sendagi, Bunkyo-ku, Tokyo 113-8602, Japan. E-mail: taknemo@nms.ac.jp.

This study was supported in part by grants from Research on Measures for Intractable Diseases; Health and Labor Sciences Research Grants from the Ministry of Health and Labor; the Ministry of Education, Culture, Sports, Science, and Technology-supported program for the Strategic Research Foundation at Private Universities, 2008–2012; and JSPS KAKENHI Grant 23791238.

Disclosure Summary: The authors have nothing to disclose.

References

1. **Birnberg NC, Lissitzky JC, Hinman M, Herbert E.** Glucocorticoids regulate proopiomelanocortin gene expression in vivo at the levels of transcription and secretion. *Proc Natl Acad Sci U S A*. 1983;80:6982–6986.
2. **Kovács KJ, Mezey E.** Dexamethasone inhibits corticotropin-releasing factor gene expression in the rat paraventricular nucleus. *Neuroendocrinology*. 1987;46:365–368.
3. **Ochedalski T, Rabadan-Diehl C, Aguilera G.** Interaction between glucocorticoids and corticotropin releasing hormone (CRH) in the regulation of the pituitary CRH receptor in vivo in the rat. *J Neuroendocrinol*. 1998;10:363–369.
4. **Childs GV, Morell JL, Niendorf A, Aguilera G.** Cytochemical studies of corticotropin-releasing factor (CRF) receptors in anterior lobe corticotropes: binding, glucocorticoid regulation, and endocytosis of [biotinyl-Ser1]CRF. *Endocrinology*. 1986;119:2129–2142.
5. **Schwartz J, Billestrup N, Perrin M, Rivier J, Vale W.** Identification of corticotropin-releasing factor (CRF) target cells and effects of dexamethasone on binding in anterior pituitary using a fluorescent analog of CRF. *Endocrinology*. 1986;119:2376–2382.
6. **Hauger RL, Millan MA, Catt KJ, Aguilera G.** Differential regulation of brain and pituitary corticotropin-releasing factor receptors by corticosterone. *Endocrinology*. 1987;120:1527–1533.
7. **Zhou Y, Spangler R, LaForge KS, Maggos CE, Ho A, Kreek MJ.** Modulation of CRF-R1 mRNA in rat anterior pituitary by dexamethasone: correlation with POMC mRNA. *Peptides*. 1996;17:435–441.
8. **Iredale PA, Duman RS.** Glucocorticoid regulation of corticotropin-releasing factor1 receptor expression in pituitary-derived AtT-20 cells. *Mol Pharmacol*. 1997;51:794–799.
9. **Rabadan-Diehl C, Makara G, Kiss A, Zelena D, Aguilera G.** Regulation of pituitary corticotropin releasing hormone (CRH) receptor mRNA and CRH binding during adrenalectomy: role of glucocorticoids and hypothalamic factors. *J Neuroendocrinol*. 1997;9:689–697.
10. **Carthew RW, Sontheimer EJ.** Origins and mechanisms of miRNAs and siRNAs. *Cell*. 2009;136:642–655.
11. **Ruvkun G.** The perfect storm of tiny RNAs. *Nat Med*. 2008;14:1041–1045.
12. **Kim YK, Heo I, Kim VN.** Modifications of small RNAs and their associated proteins. *Cell*. 2010;143:703–709.
13. **Nemoto T, Iwasaki-Sekino A, Yamauchi N, Shibasaki T.** Role of urocortin 2 secreted by the pituitary in the stress-induced suppression of luteinizing hormone secretion in rats. *Am J Physiol Endocrinol Metab*. 2010;299:E567–E575.
14. **Arai K, Ohata H, Shibasaki T.** Non-peptidic corticotropin-releasing hormone receptor type 1 antagonist reverses restraint stress-induced shortening of sodium pentobarbital-induced sleeping time of rats: evidence that an increase in arousal induced by stress is mediated through CRH receptor type 1. *Neurosci Lett*. 1998;255:103–106.
15. **Nemoto T, Iwasaki-Sekino A, Yamauchi N, Shibasaki T.** Regulation of the expression and secretion of urocortin 2 in rat pituitary. *J Endocrinol*. 2007;192:443–452.
16. **Nolan T, Hands RE, Bustin SA.** Quantification of mRNA using real-time RT-PCR. *Nat Protoc*. 2006;1:1559–1582.
17. **Shibasaki T, Kiyosawa Y, Masuda A, et al.** Distribution of growth hormone-releasing hormone-like immunoreactivity in human tissue extracts. *J Clin Endocrinol Metab*. 1984;59:263–268.
18. **Tran U, Zakin L, Schweickert A, et al.** The RNA-binding protein bicaudal C regulates polycystin 2 in the kidney by antagonizing miR-17 activity. *Development*. 2010;137:1107–1116.
19. **Kanno T, Suga S, Nakano K, Kamimura N, Wakui M.** Corticotropin-releasing factor modulation of Ca^{2+} influx in rat pancreatic β-cells. *Diabetes*. 1999;48:1741–1746.
20. **Zmijewski MA, Sharma RK, Slominski AT.** Expression of molecular equivalent of hypothalamic-pituitary-adrenal axis in adult retinal pigment epithelium. *J Endocrinol*. 2007;193:157–169.
21. **Nakakura T, Soda A, Unno K, Suzuki M, Tanaka S.** Expression of IGFBP7 mRNA in corticotrophs in the anterior pituitary of adrenalectomized rats. *J Histochem Cytochem*. 2010;58:969–978.
22. **Wang TY, Chen XQ, Du JZ, Xu NY, Wei CB, Vale WW.** Corticotropin-releasing factor receptor type 1 and 2 mRNA expression in the rat anterior pituitary is modulated by intermittent hypoxia, cold and restraint. *Neuroscience*. 2004;128:111–119.
23. **Wynn PC, Harwood JP, Catt KJ, Aguilera G.** Regulation of corticotropin-releasing factor (CRF) receptors in the rat pituitary gland: effects of adrenalectomy on CRF receptors and corticotroph responses. *Endocrinology*. 1985;116:1653–1659.
24. **Lee Y, Kim M, Han J, et al.** MicroRNA genes are transcribed by RNA polymerase II. *EMBO J*. 2004;23:4051–4060.
25. **Borchert GM, Lanier W, Davidson BL.** RNA polymerase III transcribes human microRNAs. *Nat Struct Mol Biol*. 2006;13:1097–1101.
26. **Dieci G, Fiorino G, Castelnuovo M, Teichmann M, Pagano A.** The expanding RNA polymerase III transcriptome. *Trends Genet*. 2007;23:614–622.
27. **Potter E, Sutton S, Donaldson C, et al.** Distribution of corticotropin-releasing factor receptor mRNA expression in the rat brain and pituitary. *Proc Natl Acad Sci U S A*. 1994;91:8777–8781.
28. **Wong ML, Licinio J, Pasternak KI, Gold PW.** Localization of corticotropin-releasing hormone (CRH) receptor mRNA in adult rat brain by in situ hybridization histochemistry. *Endocrinology*. 1994;135:2275–2278.
29. **Liu L, Shao X, Gao W, et al.** MicroRNA-133b inhibits the growth of non-small-cell lung cancer by targeting the epidermal growth factor receptor. *FEBS J*. 2012;279:3800–3812.
30. **Hansen TF, Andersen CL, Nielsen BS, et al.** Elevated microRNA-126 is associated with high vascular endothelial growth factor re-

The Endocrine Society. Downloaded from press.endocrine.org by [${individualUser.displayName}] on 20 January 2014. at 21:24 For personal use only. No other uses without permission. . All rights reserved.